

# Molten salt synthesis of PZT powder for direct write inks

Francesca Bortolani, Robert A. Dorey\*

*Microsystems & Nanotechnology Centre, Building 30, School of Applied Science, Cranfield University, College Road, Cranfield, Bedfordshire MK43 0AL, UK*

Received 11 November 2009; received in revised form 18 March 2010; accepted 1 April 2010

Available online 28 April 2010

## Abstract

The preparation of lead zirconate titanate (PZT) powder by molten salt synthesis (MSS) is described and a mechanism proposed. The effect of process parameters, such as reaction time and temperature and heating rate, on particle size and shape was investigated. A reaction mechanism for the synthesis of PZT by molten salt method is proposed, where dissolved Pb initially reacts with insoluble  $\text{TiO}_2$  to form intermediate  $\text{PbTiO}_3$ . Subsequently Zr diffuses into and reacts with  $\text{PbTiO}_3$  to form PZT. Spherical particles,  $\sim 340$  nm in size, were obtained, using a NaCl/KCl salt, by heating the starting materials at  $850^\circ\text{C}$  for 60 min, with a ramp rate of  $3.3^\circ\text{C min}^{-1}$ .

© 2010 Elsevier Ltd. All rights reserved.

**Keywords:** B. Grain size; D. PZT; Power-molten salt synthesis

## 1. Introduction

Lead zirconate titanate (PZT) is a versatile material widely used in micro-electro mechanical systems (MEMS). Within these MEMS the PZT takes the form of patterned films with thicknesses ranging up to  $100\ \mu\text{m}$ . Several techniques have been used to deposit ceramic thick films onto silicon substrates and create MEMS, including screen printing and photolithography.<sup>1</sup> Much attention is now focused on the miniaturization of flexible direct write technologies, such as ink jet printing (IJP). These techniques allow the creation of microscale 3D structures under computer control<sup>2–4</sup> and provide advantages over the common microprocessing techniques, including high printing speed, direct patterning capability, absence of harsh etchants, low material wastage and high resolution. This leads to a more environmentally friendly and flexible process. In order for an IJP ink to perform, the ceramic particles within the ink should be less than 1/100 of the diameter of the printing nozzles in order to prevent clogging and allow “clean” droplet ejection. Hence for current high resolution systems, the powder should be smaller than  $\sim 200$  nm in diameter. Such small sizes are also important for obtaining stable suspensions, particularly with high density

materials such as PZT which sediment at high rates. A twofold reduction in size will result in a fourfold reduction in sedimentation rate of the powder. However, even particles in the submicron range (smaller than  $1\ \mu\text{m}$  in diameter) can be printed by IJP if a stable suspension is created.

Different synthesis routes have been studied in order to obtain PZT particles in the submicron range, including electro hydro dynamic atomization (EHDA),<sup>5</sup> sol-gel<sup>6–8</sup> and hydrothermal<sup>9</sup> synthesis. EHDA leads to the production of small and spherical particles, but the yield is very low. Sol-gel and hydrothermal synthesis are usually long and complex processes, use hazardous solvents such as 2-methoxyethanol, and result in agglomerated particles or large particles not suitable for ink jet printing. In order to overcome these problems, molten salt synthesis (MSS) has been investigated for the production of PZT powder to obtain spherical particles in the submicron range.

MSS is a process that yields large amounts of ceramic in a relatively short period of time. In this technique starting materials are mixed together with a salt and then heat treated at a temperature higher than the melting point of the salt. The melting temperature of the salt system can be reduced by using a eutectic mixture of salts, e.g. the use of NaCl/KCl instead of pure NaCl reduces the melting point from  $801$  to  $657^\circ\text{C}$ . A reaction between the precursors takes place in the molten salt (the flux) and the solid product obtained is separated by washing of the final mixture with hot deionised water. The typical starting

\* Corresponding author.

E-mail addresses: [f.bortolani@cranfield.ac.uk](mailto:f.bortolani@cranfield.ac.uk) (F. Bortolani), [r.a.dorey@cranfield.ac.uk](mailto:r.a.dorey@cranfield.ac.uk) (R.A. Dorey).

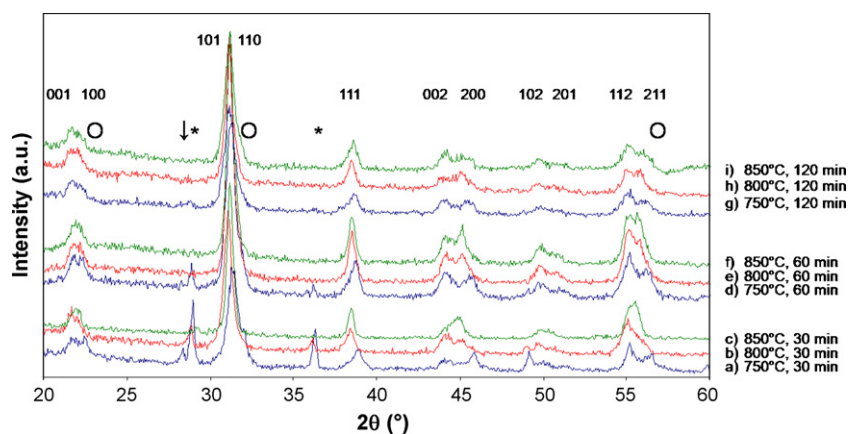


Fig. 1. XRD patterns of PZT powders produced using MSS at different temperatures and for different dwell times. Temperature ramp rate of  $20^{\circ}\text{C min}^{-1}$ . The symbols  $\circ$ ,  $*$  and  $\downarrow$  indicate peaks related to  $\text{PbTiO}_3$ ,  $\text{PbO}$  and  $\text{ZrO}_2$ , respectively.

materials are oxides, but oxalates, nitrates and carbonates can also be used.<sup>10–13</sup>

The salt plays an important role in the synthesis process, because the atomic mobility of the reacting species in the molten salt is higher than the mobility in solid state reactions.<sup>14</sup> This allows the reaction to be completed in a shorter period of time. The salt, or the mixture of salts, is selected to: (a) not react with the starting materials or the product; (b) be soluble in water in order to be removed easily by washing; (c) have a relatively low melting point.<sup>11,14,15</sup> Several complex oxide ceramics have been synthesized by this method, including potassium sodium niobate,<sup>16</sup>  $\text{BaZrO}_3$ <sup>12,13,17</sup> and lead-based compounds, such as lead lanthanum zirconate titanate,<sup>10</sup> lead lanthanum zirconate titanate stannate,<sup>18</sup> lead titanate<sup>19</sup> and lead ferroniobate.<sup>15,20</sup> The effects of the MSS processing parameters on the particle size have previously been experimentally investigated, yet no mechanism has been proposed. In these studies it was noted that longer reaction times led to an increase in the particle size<sup>12,13,15</sup> and greater product purity.<sup>12,13</sup> Higher temperatures help to obtain a pure product and to increase the formation of nuclei,<sup>13,20</sup> which results in a higher number of particles. On the other hand it

also results in an increase in particle size.<sup>12,15,21</sup> A reduction of the particle dimension can be achieved by increasing the rate of heating to the reaction temperature.<sup>15</sup> Another parameter that has an effect on the final product is the salt-to-reactants ratio. Yoon et al.<sup>15</sup> and Zhou et al.<sup>12</sup> noticed that a higher ratio led to bigger particles. It should be noted that with a smaller ratio it is simpler to remove the salt. These observations indicate that to obtain small particles by MSS it is necessary to employ a short time, low temperature and fast heating rate with a low salt quantity.

Based on this hypothesis, the aim of this work was to develop an understanding of the mechanism of MSS within this regime and to synthesize equiaxed or spherical PZT (Zr:Ti ratio of 0.5:0.5) powder in the submicron range for the development of an ink suitable for high resolution ink jet printing.

## 2. Experimental procedure

PZT powder was prepared by molten salt synthesis using metal oxides as starting materials: lead, zirconium and titanium oxides.  $\text{NaCl}$  and  $\text{KCl}$ , in the eutectic molar ratio of 1:1 were

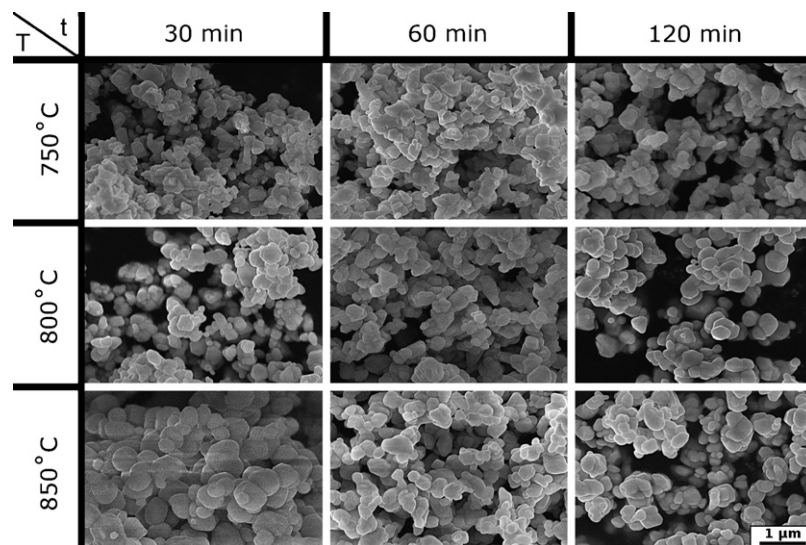


Fig. 2. SEM micrographs of PZT powders synthesized at different temperatures and for different isothermal times, with a temperature ramp rate of  $20^{\circ}\text{C min}^{-1}$ .

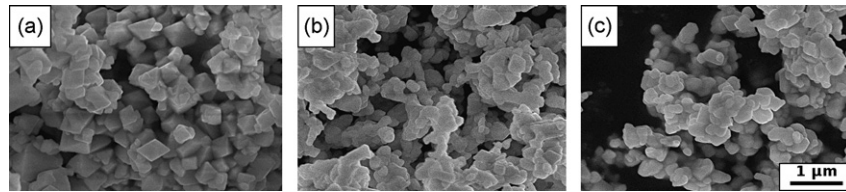


Fig. 3. SEM micrographs of PZT powders synthesized at 750 °C, with a temperature ramp rate of 5 °C min<sup>-1</sup> for different isothermal times: (a) 30, (b) 60 and (c) 120 min.

used as the reaction flux. A slurry containing stoichiometric amounts of the starting materials was ball milled with the flux (1:1 by weight) for 24 h with ethanol as the carrier. Following mixing, the slurry was dried overnight at 100 °C to remove the ethanol. All the starting materials, except PbO were obtained from Sigma–Aldrich, with purity higher than 99%. PbO was instead obtained from BDH and its purity was 98%.

The resultant mixture was heat treated in an open alumina crucible at temperatures between 750 and 850 °C. The temperature ramp rates were set at 3.3, 5, 10, 20 or 70 °C min<sup>-1</sup>. The time of the reaction (isothermal time) was varied from 30 min to 2 h.

After synthesis the powder was washed with deionised water at approximately 60 °C, until no Cl<sup>-</sup> ions were observable in the filtered water, as tested by adding AgNO<sub>3</sub> solution. The PZT powder was dried at 80 °C overnight and then ground by mortar and pestle to break up the loose agglomerates resulting from the water evaporation.

The crystallinity of the synthesized powders was investigated by X-ray diffraction (XRD, D5005 Siemens). The morphology was investigated by scanning electron microscopy (SEM SFEG XL30, FEI).

### 3. Results

Fig. 1 represents the XRD patterns of the powders synthesized for different periods of time (30, 60 and 120 min) at 750, 800 and 850 °C with a temperature ramp rate of 20 °C min<sup>-1</sup>. Similar trends were also observed for PZT produced using other heating rates.

PZT perovskite phase was observed in all the samples. In the XRD patterns of the powders that were reacted for 30 min at all temperatures and for 60 min at 750 °C (Fig. 1d) additional peaks at approximately 29° and 36° 2θ were detected. These can be attributed to the presence of unreacted PbO. SEM analysis showed evidence of large Pb rich particles within the resultant powders. Zirconia peaks were also detected in the sample heated quickly to 750 °C and held for 30 min but only in cases employing the fastest temperature ramp rates, such as 20

(Fig. 1a) and 70 °C min<sup>-1</sup>. Moreover in the sample heated at 750 °C for 30 min, lead titanate, PT, was also detected (symbol ○ in Fig. 1a). The slight variations in the position of the PZT peaks observed in Fig. 1 are due to slight differences in the composition of the PZT powder.

The particle morphology of the powders is compared in Fig. 2.

It can be noted that increasing the reaction temperature (top to bottom) or time (left to right) led to an increase in the particle size. This is more evident for powders synthesized for shorter isothermal times (30 min). The shape gradually became more regular with increasing isothermal time (left to right). Both the phenomena were also observed at lower heating ramp rates (Figs. 3 and 4). At the lowest processing temperature and time (750 °C, 30 min) the synthesized PZT powder had a distinctive cube like shape (Fig. 3a) which became less pronounced with increasing process parameters.

### 4. Discussion

The observations that particle size increases with increasing temperature and time can be accounted for by considering the processes occurring during molten salt synthesis.

The MSS mechanism is a two-step process consisting of particle nucleation and subsequent coarsening.<sup>22</sup> The coarsening can occur in two ways. In the first one the particles grow by the addition of new material from the salt solution. With time the number of particles does not change but they grow in size. In the second way the large particles grow and the small ones dissolve (Ostwald ripening).<sup>23</sup> Hence a longer isothermal time should lead to fewer but larger particles. An increase in temperature also increases the time at which the flux is in the liquid state as the overall reaction time (the time during which the flux is liquid) is the sum of the isothermal time and the time taken to reach the required temperature once the melting point of the salt has been attained. Moreover the mobility of the atomic species in the salt is higher at higher temperatures meaning they can diffuse more rapidly through the flux and react thereby producing bigger PZT particles (Fig. 4).

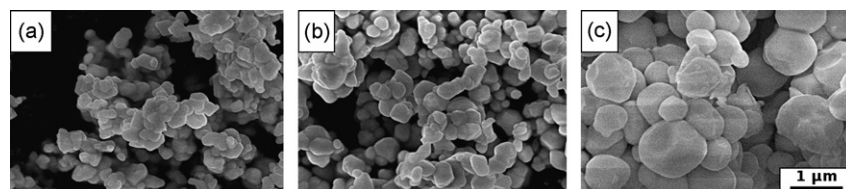


Fig. 4. SEM micrographs of PZT powders synthesized for 120 min at (a) 750, (b) 800 and (c) 850 °C, using a ramp rate of 5 °C min<sup>-1</sup>.



Yoon et al.<sup>15</sup> noted that the heating profile also influences the final particle size and size distribution of lead manganese niobate. They showed that the average particle size was reduced from  $\sim 1.5$  to  $\sim 0.5 \mu\text{m}$  by increasing the heating rate from 5 to  $150 \text{ }^\circ\text{C min}^{-1}$ . The size reduction of PMN was noticed in the synthesis conducted with a  $\text{Li}_2\text{SO}_4/\text{Na}_2\text{SO}_4$  mixture. The authors suggested that in this solvent a dissolution–precipitation mechanism occurred due to the high solubility of the starting materials in sulphates. This behaviour was not noticed in our tests, but it was instead observed that a change in the particle shape occurred, with particles becoming more regular with decreasing ramp rates (at constant isothermal time and temperature). Moreover an increment in the heating rate led to a larger particle size distribution, with the presence of big particles in the final PZT powder. This correlates with the observed results, and predicts that for small particles to be obtained short time and low temperatures should be favoured.

At short isothermal times (30 min) the particle shape was irregular and gradually changed into a more spherical shape with increasing time, as can be seen in Figs. 2 and 3. This is similar to what has been shown by Zhou et al.<sup>12,13</sup> in the synthesis of  $\text{BaZrO}_3$  particles. They noted that cubes of  $\text{BaZrO}_3$  precipitated from the mixture. Over time, the cubes were gradually transformed into spheres by the coarsening process.

The solubility of the starting materials in the molten salt plays an important role in the synthesis as it has an influence on the final product morphology and on the reaction rate.<sup>19</sup> For a simple two reactant system ( $\text{AO} + \text{BO}$ ), two different cases can be distinguished: either both reactants are equally soluble in the molten salt or one oxide is more soluble than the other.<sup>24</sup> In the first case (dissolution–precipitation mechanism) both reactants fully dissolve, react in the molten salt and the final product precipitates from the molten salt after formation. The shape of the

product has no connection with the shape of the starting materials. In the second case (template formation mechanism), the more soluble reactant dissolves in the salt and diffuses to the less soluble one. Here, at the surface, it reacts *in situ* to synthesize the product. This mechanism would result in a product morphology that is similar to that of the less soluble reactant which has acted as a template. In the case of PZT the mechanism is further complicated due to the presence of (at least) 3 reactants.

According to Yoon et al.<sup>15</sup>  $\text{PbO}$  solubility in chloride salts is higher than that of  $\text{ZrO}_2$ . Since  $\text{TiO}_2$  is not soluble in molten alkali chlorides,<sup>19</sup> the final PZT morphology should be similar to the morphology of  $\text{TiO}_2$  (template formation mechanism), or possibly  $\text{ZrO}_2$  where its dissolution is incomplete.

The mechanisms for formation of PZT by MSS have not been reported in literature. Reports on the formation of PZT during mixed oxide solid state reaction<sup>25,26</sup> propose that  $\text{PbO}$  diffuses into and reacts *in situ* with  $\text{TiO}_2$  particles forming a  $\text{PbTiO}_3$  shell around a  $\text{TiO}_2$  core. PT then reacts further with  $\text{PbO}$  and  $\text{ZrO}_2$  to form PZT. In the case of zinc aluminate solid state synthesis it was determined that the rate-controlling step is the diffusion of Zn ions through the  $\text{ZnAl}_2\text{O}_4$  shell<sup>27</sup> (i.e. rate is limited by the fastest route of the slowest diffusing species).

In the case of MSS of PZT, Pb is a very mobile species so the formation of PT should be quick. To produce PZT, Zr then has to diffuse into and react with the PT. It is reasonable to suppose that in the case of PZT the rate-controlling stage is therefore the diffusion of the remnant ions (Zr) through the PT as with Zn in the case of  $\text{ZnAl}_2\text{O}_4$  synthesis. This reaction system and the template formation mechanism can be used to explain the observed formation of PZT particles in molten salt synthesis. In the early stage of the process residual  $\text{PbO}$  and  $\text{ZrO}_2$ , along with the intermediate PT should all be detected along side PZT. In the samples synthesized at low temperature, low isothermal

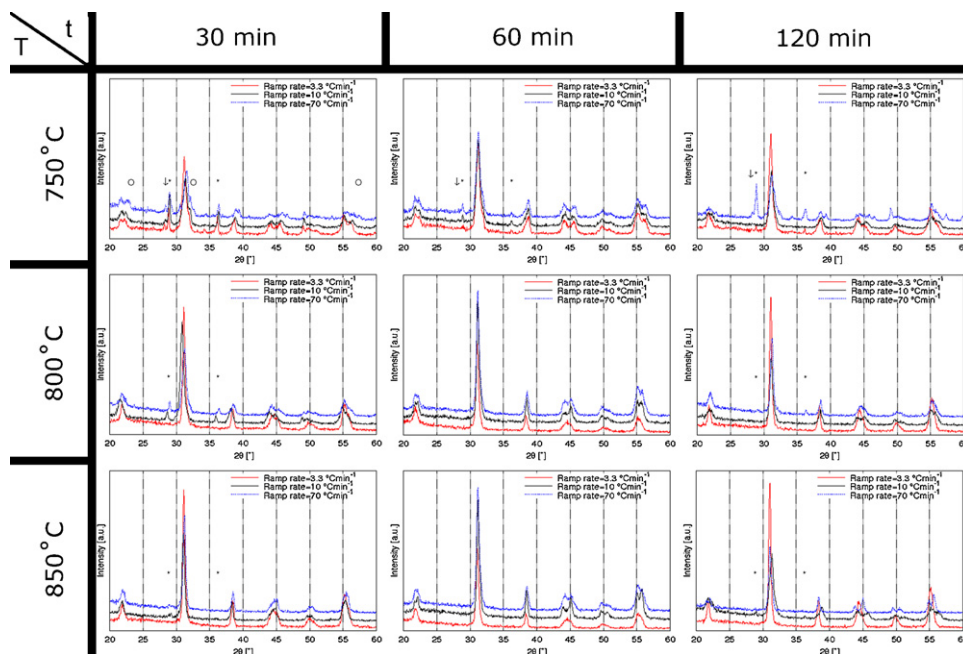


Fig. 5. XRD patterns of PZT powders heated at 3.3, 10 and  $70 \text{ }^\circ\text{C min}^{-1}$  to 750, 800 and  $850 \text{ }^\circ\text{C}$  for 30, 60 and 120 min. The symbols \*, ↓ and ○ indicate peaks related to  $\text{PbO}$ ,  $\text{ZrO}_2$  and  $\text{PbTiO}_3$ , respectively.

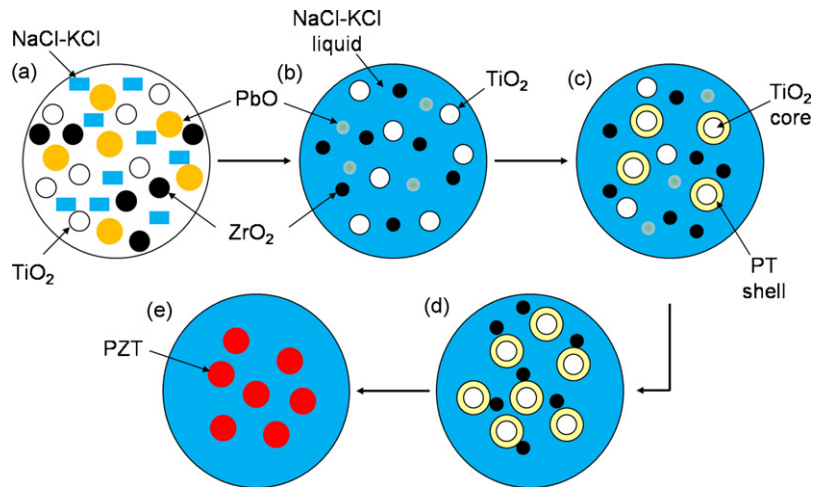
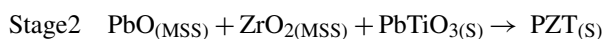
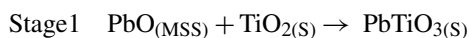


Fig. 6. Schematic representation of the synthesis of PZT in molten salt: (a) PbO, ZrO<sub>2</sub>, TiO<sub>2</sub> and solid NaCl/KCl, (b) PbO completely dissolved and partial dissolution of ZrO<sub>2</sub>, (c) PT shell formation, (d) diffusion of Zr and (e) PZT formation.

time and fast ramp rate, such as 20 (Fig. 1a) or 70 °C min<sup>-1</sup>, the presence of these oxides was indeed detected. As the reaction proceeds the TiO<sub>2</sub> should be completely consumed to produce PT, leaving only residual PbO and ZrO<sub>2</sub>. In Fig. 5 the XRD patterns of PZT powders synthesized at 750, 800 and 850 °C for 30, 60 and 120 min under 3.3, 10 and 70 °C min<sup>-1</sup> heating rates are shown. These ramp rates were chosen in order to represent the powder synthesized at the lowest, highest and medium ramp rates. When the samples were heated at 750 °C for 30 min, residual PbO and ZrO<sub>2</sub> were detected. If fast ramp rates, such as 20 or 70 °C min<sup>-1</sup>, were used to heat the samples, peaks of PT were also observed in the XRD patterns. As the time was increased to 60 min (at the same temperature) PbO was detected in all the samples, but ZrO<sub>2</sub> only in the samples heated at 20 or 70 °C min<sup>-1</sup>. A further increase in the isothermal time led the reaction to proceed and PbO and ZrO<sub>2</sub> were detected only in the sample heated at 70 °C min<sup>-1</sup>. However, residual PbO was found in the sample heated at 3.3 °C min<sup>-1</sup> at the same time and temperature, meaning an incomplete reaction. When the reaction temperature was increased to 800 °C no more ZrO<sub>2</sub> peaks were observed in the XRD patterns. This means that a reaction had occurred. PbO was still present in the samples heated at 10, 20 and 70 °C min<sup>-1</sup> to 800 °C for 30 min or for 120 min (only at 70 °C min<sup>-1</sup>). PbO was detected again after 30 min of reaction at 850 °C in the cases where 5, 10, 20 or 70 °C min<sup>-1</sup> were used as heating ramps. At higher isothermal times PbO was found only in the sample heated at 10 °C min<sup>-1</sup>.

The observations indicate that all the TiO<sub>2</sub> has reacted with PbO (stage 1) yet residual ZrO<sub>2</sub> and PbO are still present (stage 2) due to the lower diffusivity of the Zr species. The reaction process can be represented schematically by Fig. 6.



The formation of cubic particles at 750 °C (isothermal time of 30 min) can also be explained by considering the growth mech-

anism of the PZT. The TiO<sub>2</sub> starting particles are small and mostly consist of single crystallites. In the early stages of growth, incoming material is likely to deposit and react on preferential growth planes, leading to the cuboid shape. As the particle continues to grow, other forces, such as surface energy, will favour the formation of more equiaxed particles. In Fig. 7 the starting TiO<sub>2</sub> and the final spherical PZT powders obtained by heating the starting oxides and the salts at 3.3 °C min<sup>-1</sup> at 850 °C for 60 min are compared. It can be seen that the morphology of the synthesized PZT is similar to that of the TiO<sub>2</sub>, with the PZT particles being larger than TiO<sub>2</sub>. The different dimension of the particles can be interpreted as a consequence of the addition of ZrO<sub>2</sub> and PbO to form PZT (grain growth).

In order to identify if the grains coarsen, a rough size calculation can be made. In the absence of coarsening, and assuming that the PZT particles will only be larger than the TiO<sub>2</sub> ones due to the addition of Pb and Zr an initial 160 nm TiO<sub>2</sub> particles, should result in PZT particles of about 260 nm in diameter. Since all the PZT particles in our tests were larger than 260 nm, it is possible to assume that coarsening has occurred most importantly by Oswald ripening of particles in close proximity. Fig. 7b shows evidence of particles that appear to have fused together during processing.

To obtain small PZT particles a compromise between low temperature and short time is needed. Fig. 8 is a schematic representation of the changes in particle size (circles) with time and temperature. At low time and temperature (bottom left area) the presence of residual PbO and ZrO<sub>2</sub> and PT was detected. When the starting materials were reacting for long time at high temperature, large particles were created instead. The smallest PZT particles (star in Fig. 8) were obtained by heating the mixture at 850 °C for 60 min with a temperature ramp rate of 3.3 °C min<sup>-1</sup>. Almost spherical particles with diameters of ~340 nm were synthesized under these conditions.

Since the assumptions are that PZT grows from TiO<sub>2</sub> that is not dissolved in the molten salt and the rate limiting step is the diffusion of Zr into PT, several aspects can be considered in order to achieve small PZT particles. Principally the PZT forma-

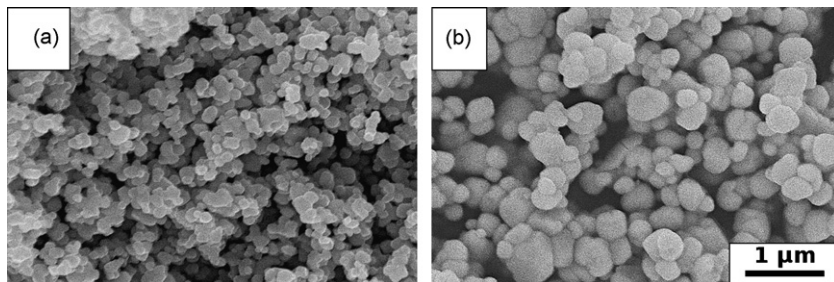


Fig. 7. SEM micrograph of TiO<sub>2</sub> (a) and PZT powder synthesized at 850 °C for 60 min (heating ramp 3.3 °C min<sup>-1</sup>) (b).

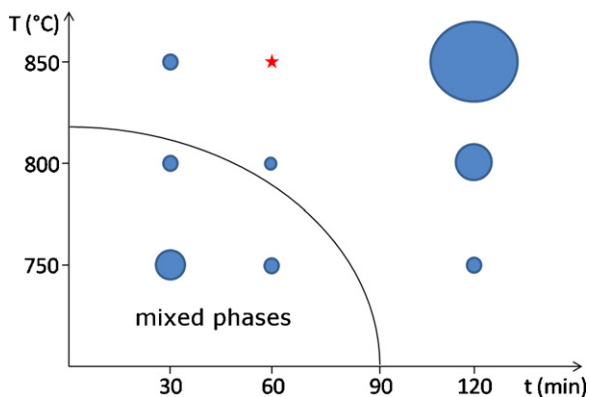


Fig. 8. Schematic representation of particle size as a function of temperature and isothermal time.

tion mechanism needs to be enhanced relative to the coarsening mechanism. This can be achieved by reducing the diffusion distance. To do so a thinner PT layer and small TiO<sub>2</sub> particles (as they do not dissolve) are needed. Nano-TiO<sub>2</sub> was prepared as described in Ref.<sup>28</sup> and the mean particle size was approximately 60 nm following crystallization at 450 °C for 1 h. The resultant PZT powder synthesized was not reduced in size as predicted and no difference in final PZT powder size was noted. It was instead observed that individual particles were fused together. This indicates that while small particles were produced, the enhanced sintering driving force of the small PZT/nano-TiO<sub>2</sub> also led to agglomeration and coarsening.

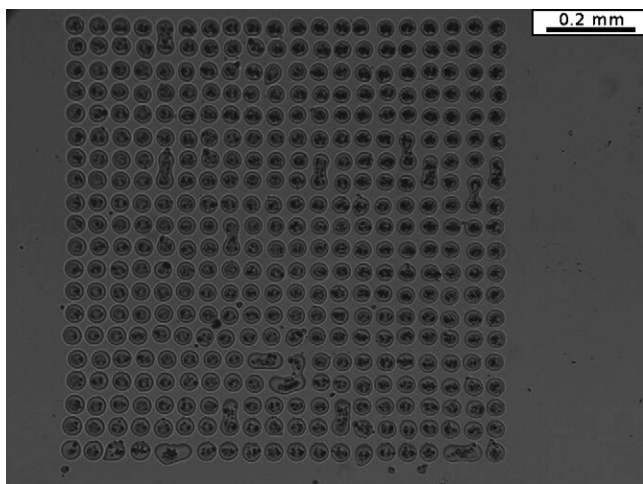


Fig. 9. Optical micrograph of the 20 × 20 dots pattern printed with 1 vol% ink under the following conditions: voltage 16 V, CPH 0.35 mm and 1 nozzle.

The final purpose of this work was to synthesize PZT particles suitable for ink jet printing. The particles should be 1/100 of the printing nozzle diameter, that means smaller than ~200 nm in diameter. The PZT particles obtained by MSS were larger than the required size, but an ink composed of 1 vol% of powder in PZT sol was prepared. An additional 1.5 wt% (with respect to the powder amount) of dispersant (KR-55) was added to the formulation in order to maintain the particles in suspension. After dispersion of the components by the use of an ultrasonic horn, the ink was successfully printed by a Fujifilm Dimatix ink jet printer onto silicon substrate, as shown in Fig. 9. A pattern composed of 20 × 20 drops was printed with a firing voltage of 16 V, a distance between the cartridge and the substrate (CPH) of 0.35 mm and with 1 nozzle.

## 5. Conclusions

At shorter times (30 min) the reaction between the starting materials was not complete. Residual PbO and ZrO<sub>2</sub> and PT were found within the product. The particles obtained at 750 °C and at fast heating rates were less spherical than the same powder treated at higher temperatures for the same isothermal time. At high temperatures and long reaction times an excessive particle growth was observed. The smallest particles were obtained by heating the raw materials at 850 °C for 60 min using a slow temperature ramp rate (3.3 °C min<sup>-1</sup>). The final PZT had an average particle size of ~340 nm. A molten salt mechanism for the formation of PZT is proposed whereby dissolved Pb initially reacts with the insoluble TiO<sub>2</sub> particles to form PbTiO<sub>3</sub>. Dissolved Zr then diffuses into the PbTiO<sub>3</sub> forming PZT. The diffusion of Zr through the PbTiO<sub>3</sub> is the rate limiting stage. At the same time as the Zr diffusion, particle coarsening (through particle coalescence) occurs revealing a challenge to create small particles where two low solubility phases are present.

The synthesized PZT powder was dispersed into a PZT sol in order to create an ink suitable for ink jet printing. The suspension was successfully printed onto silicon substrates demonstrating the possibility of using ink jet printing technology for the creation of microscale structures.

## Acknowledgements

The authors would like to thank the financial support from the Engineering and Physical Sciences Research Council via the project “Low temperature micromoulding of functional ceramic

devices” (GR/S84156/01) and the European Commission via the project “Multifunctional & Integrated Piezoelectric Devices” (NoE 515757-2).

## References

- Dorey RA, Whatmore RW. Electroceramic thick film fabrication for MEMS. *J Electroceram* 2004;**12**:19–32.
- Lewis JA. Direct-write assembly of ceramics from colloidal inks. *Curr Opin Solid State Mater Sci* 2002;**6**:245–50.
- Lewis JA, Smay JE, Stuecker J, Cesarano III J. Direct ink writing of three-dimensional ceramic structures. *J Am Ceram Soc* 2006;**89**:3599–609.
- Zhao X, Evans JRG, Edirisinghe MJ, Song JH. Formulation of a ceramic ink for a wide-array drop-on-demand ink-jet printer. *Ceram Int* 2003;**29**:887–92.
- Bortolani F, Dorey RA. Synthesis of spherical lead zirconate titanate (PZT) nanoparticles by electrohydrodynamic atomisation. *Adv Appl Ceram* 2009;**108**:332–7.
- Mu G, Yang S, Li J, Gu M. Synthesis of PZT nanocrystalline powder by a modified sol–gel process using water as primary solvent source. *J Mater Process Technol* 2007;**182**:382–6.
- Linardos S, Zhang Q, Alcock JR. Preparation of sub-micron PZT particles with the sol–gel technique. *J Eur Ceram Soc* 2006;**26**:117–23.
- Fernandez-Osorio AL, Vazquez-Olmos A, Mata-Zamora E, Saniger JM. Preparation of free-standing Pb(Zr<sub>0.52</sub>Ti<sub>0.48</sub>)O<sub>3</sub> nanoparticles by sol–gel method. *J Sol Gel Sci Technol* 2007;**42**:145–9.
- Deng Y, Liu L, Cheng Y, Nan C, Zhao S. Hydrothermal synthesis and characterization of nanocrystalline PZT powders. *Mater Lett* 2003;**57**:1675–8.
- Cai Z, Xing X, Li L, Xu Y. Molten salt synthesis of lead lanthanum zirconate titanate ceramic powders. *J Alloys Compd* 2008;**454**:466–70.
- Nersisyan HH, Lee JH, Won CW. SH-synthesis of ceramic powders in the fusion salts of alkali metal. *J Ceram Process Res* 2005;**6**:41–7.
- Zhou H, Mao Y, Wong SS. Probing structure-parameter correlations in the molten salt synthesis of BaZrO<sub>3</sub> perovskite submicrometer-sized particles. *Chem Mater* 2007;**19**:5238–49.
- Zhou H, Mao Y, Wong SS. Shape control and spectroscopy of crystalline BaZrO<sub>3</sub> perovskite particles. *J Mater Chem* 2007;**17**:1707–13.
- Arendt RH, Rosolowski JH, Szymaszek JW. Lead zirconate titanate ceramics from molten salt solvent synthesized powders. *Mater Res Bull* 1979;**14**:703–9.
- Yoon KH, Cho YS, Kang DH. Molten salt synthesis of lead-based relaxors. *J Mater Sci* 1998;**33**:2977–84.
- Zeng JT, Kwok KW, Chan HLW. KxNa<sub>1-x</sub>NbO<sub>3</sub> powder synthesized by molten-salt process. *Mater Lett* 2007;**61**:409–11.
- Mao Y, Park T-, Zhang F, Zhou H, Wong SS. Environmentally friendly methodologies of nanostructure synthesis. *Small* 2007;**3**:1122–39.
- Zhao S, Li Q, Wang L, Zhang Y. Molten salt synthesis of lead lanthanum zirconate titanate stannate powders and ceramics. *Mater Lett* 2006;**60**:425–30.
- Cai Z, Xing X, Yu R, Sun X, Liu G. Morphology-controlled synthesis of lead titanate powders. *Inorg Chem* 2007;**46**:7423–7.
- Chiu CC, Li CC, Desu SB. Molten salt synthesis of a complex perovskite, Pb(Fe<sub>0.5</sub>Nb<sub>0.5</sub>)O<sub>3</sub>. *J Am Ceram Soc* 1991;**74**:38–41.
- Kimura T, Takenaka A, Mifune T, Hayashi Y, Yamaguchi T. Preparation of needle-like TiZrO<sub>4</sub> and PZT powders. *J Mater Sci* 1992;**27**:1479–83.
- Roy B, Ahrenkiel SP, Fuierer PA. Controlling the size and morphology of TiO<sub>2</sub> powder by molten and solid salt synthesis. *J Am Ceram Soc* 2008;**91**:2455–63.
- Chiang YM, Birnie DI, Kingery WD. *Physical ceramics. Principles for ceramic science and engineering*. Wiley and sons Inc.; 1997. p. 388.
- Li Z, Lee WE, Zhang S. Low-temperature synthesis of CaZrO<sub>3</sub> powder from molten salts. *J Am Ceram Soc* 2007;**90**:364–8.
- Chandratreya SS, Fulrath RM, Pask JA. Reaction mechanisms in the formation of PZT solid solutions. *J Am Ceram Soc* 1981;**64**:422–5.
- Russell VA, Spink CH. The differential thermal analysis behavior of lead zirconate titanate materials. *Thermochim Acta* 1977;**19**:45–54.
- Li Z, Zhang S, Lee WE. Molten salt synthesis of zinc aluminate powder. *J Eur Ceram Soc* 2007;**27**:3407–12.
- Chen J, Gao L, Huang J, Yan D. Preparation of nanosized titania powder via the controlled hydrolysis of titanium alkoxide. *J Mater Sci* 1996;**31**:3497–500.